

YMTHE, Volume 26

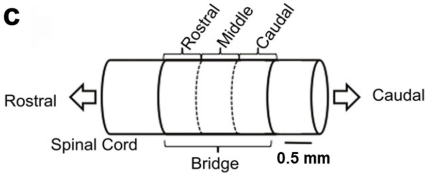
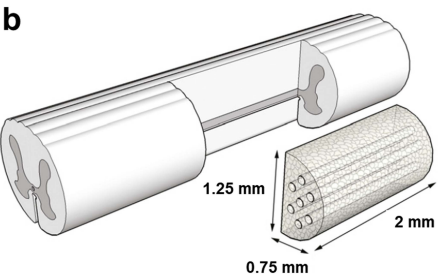
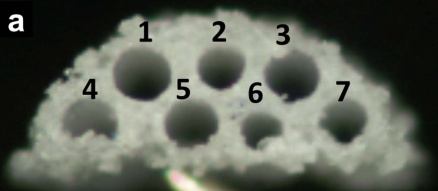
Supplemental Information

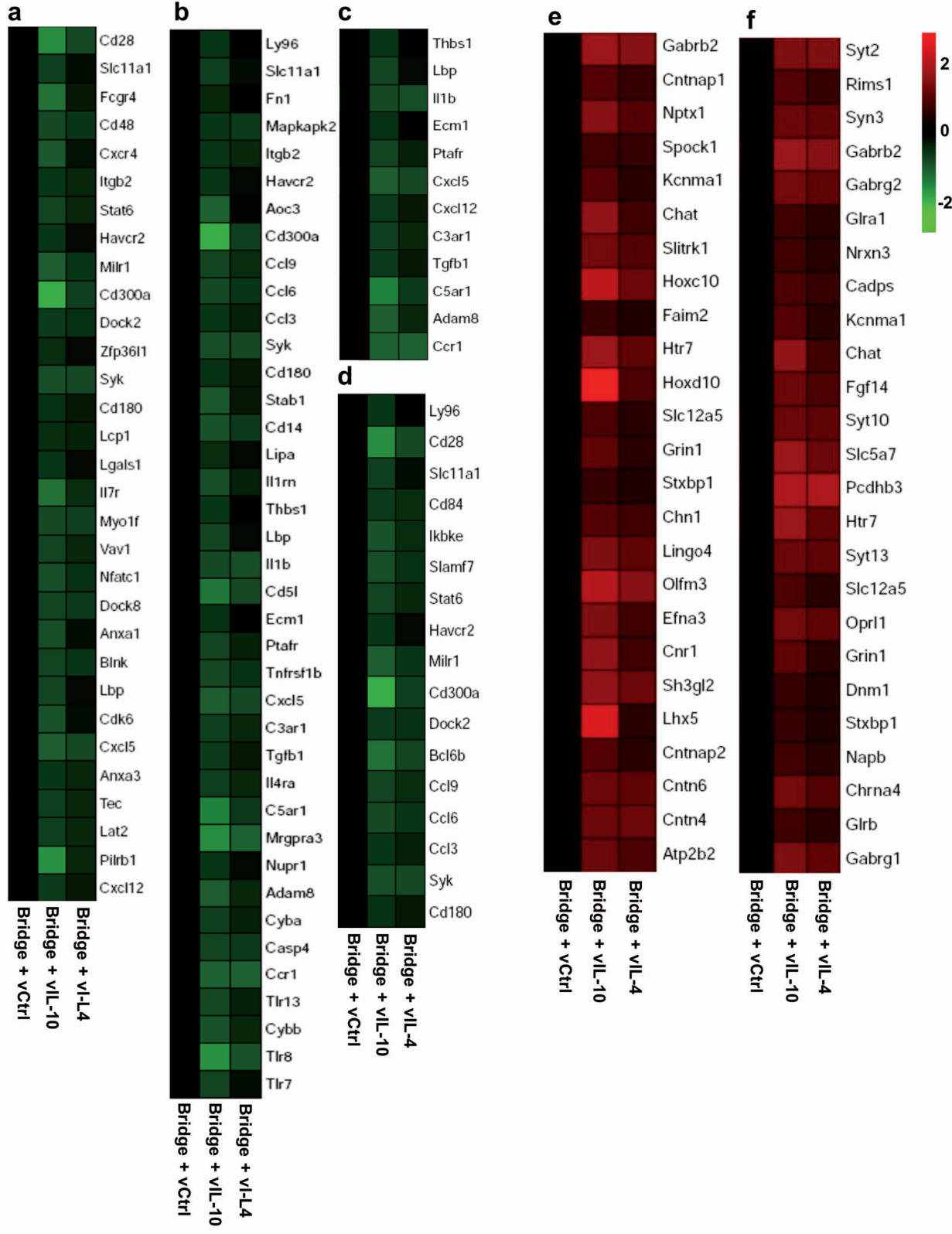
Local Immunomodulation with Anti-inflammatory

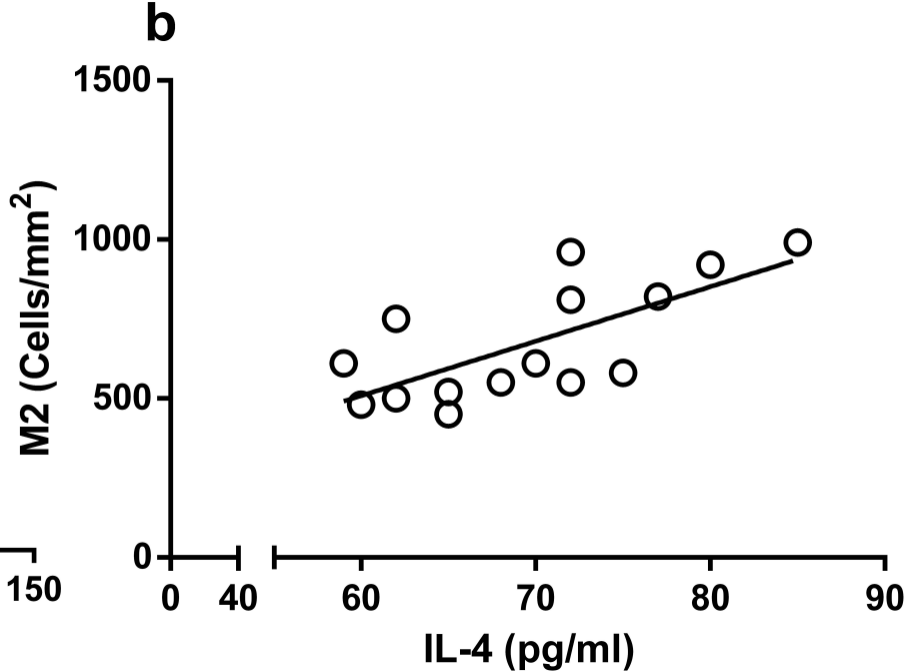
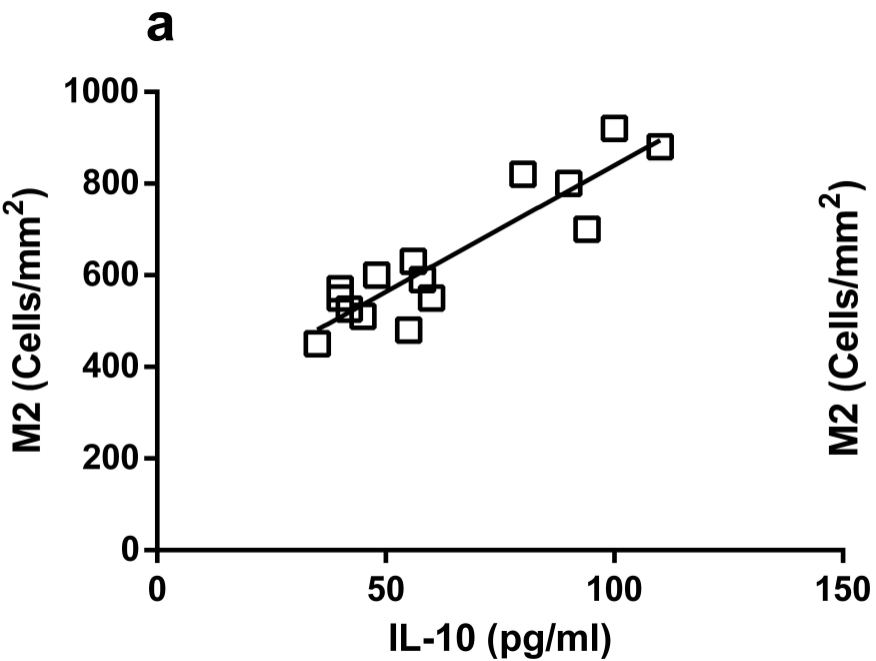
Cytokine-Encoding Lentivirus Enhances

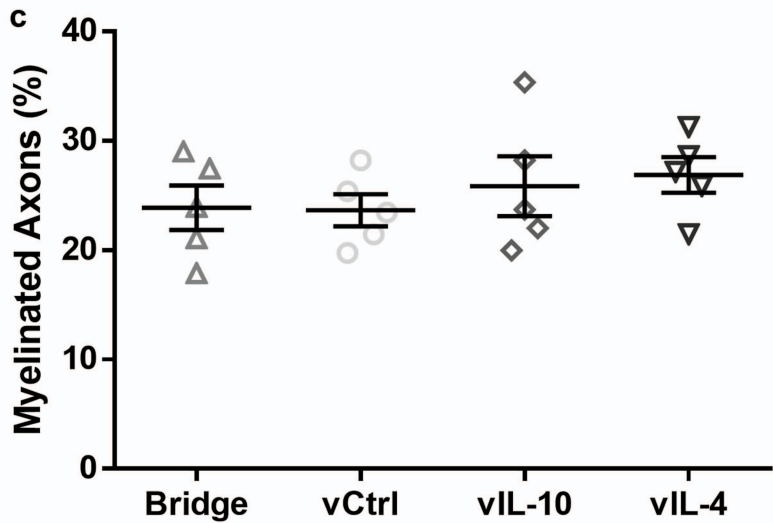
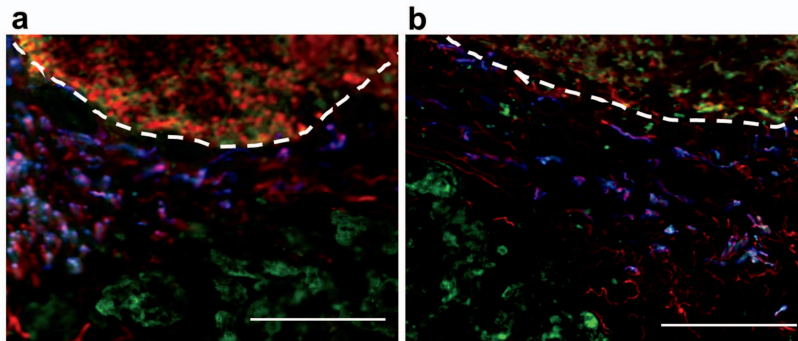
Functional Recovery after Spinal Cord Injury

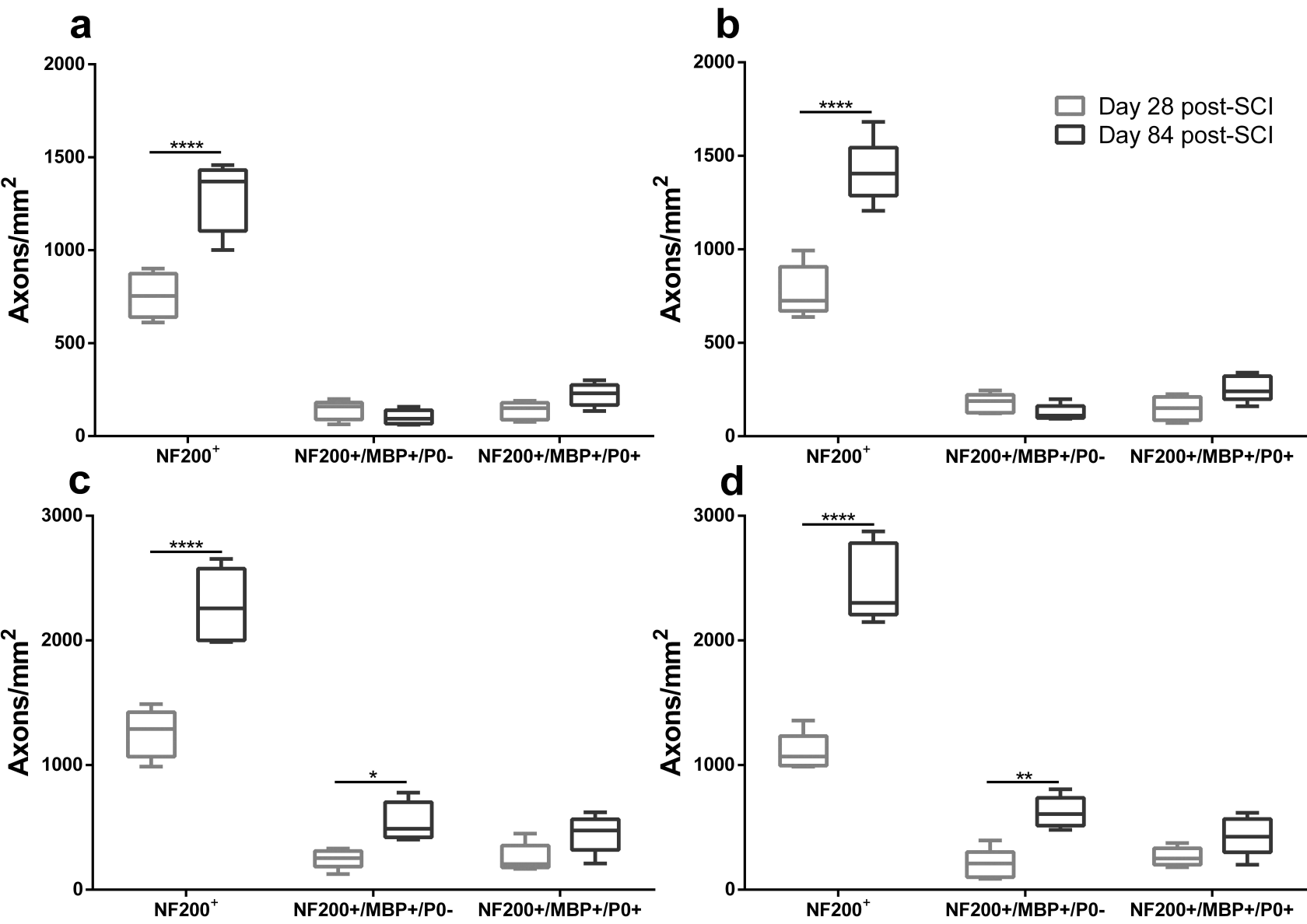
Jonghyuck Park, Joseph T. Decker, Daniel J. Margul, Dominique R. Smith, Brian J. Cummings, Aileen J. Anderson, and Lonnie D. Shea

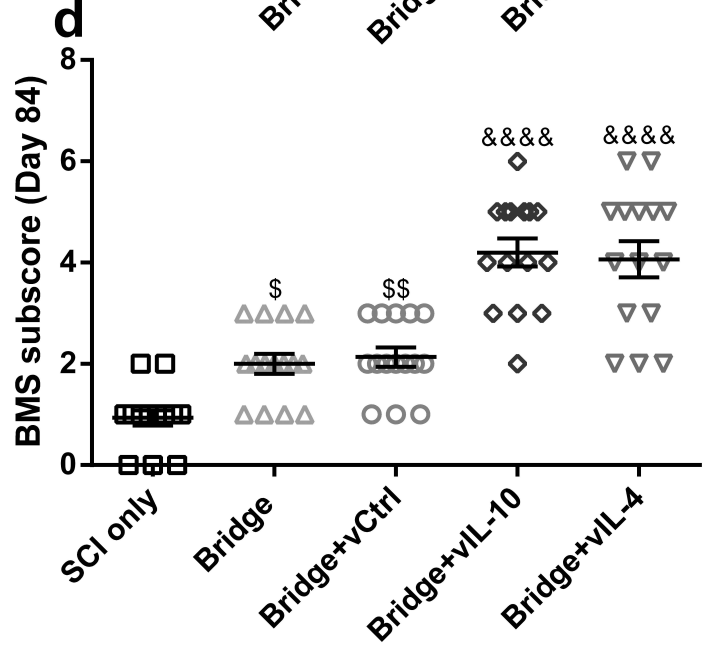
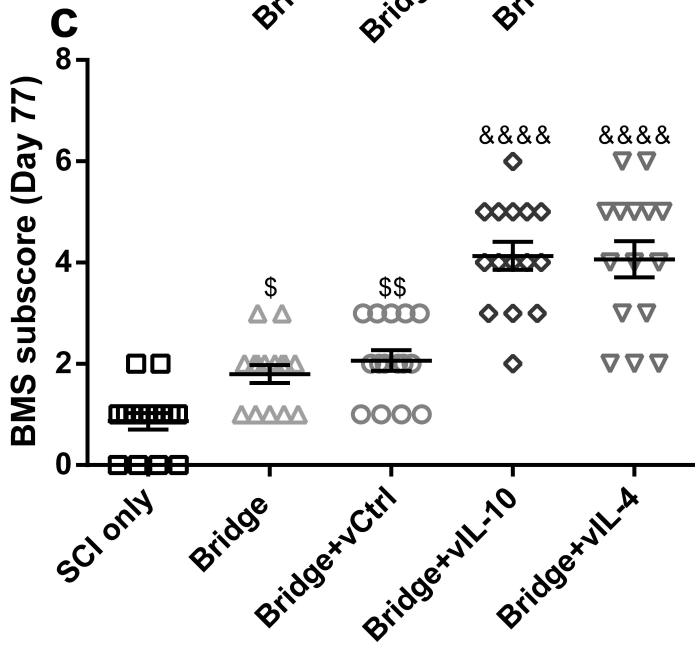
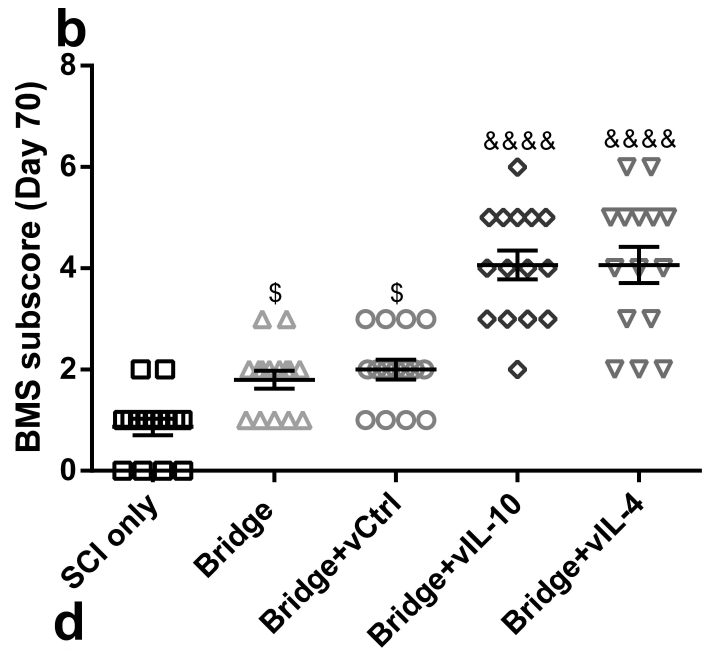
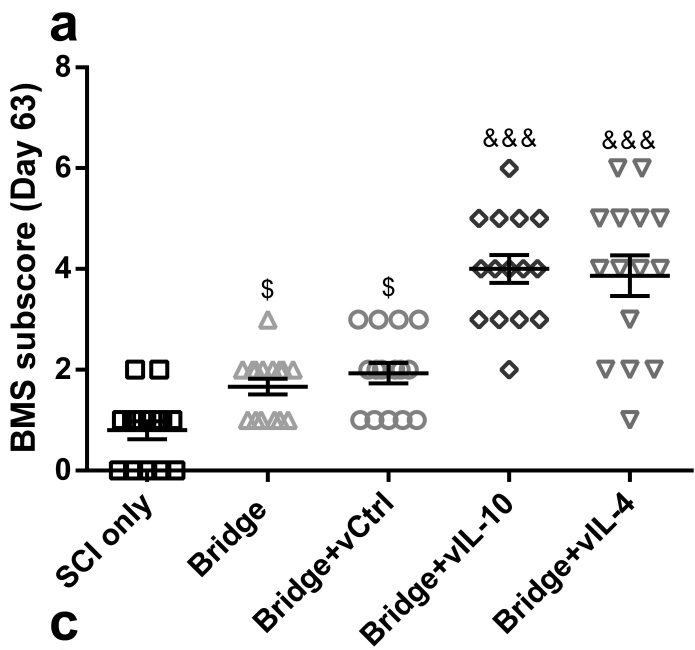












Supplemental figure legends

Figure. S1. PLG multichannel bridge and hemi-sectional SCI model. (a) Photomicrograph of a bridge with 200 μm multichannel. (b) Schematic representation of hemi-section SCI at T9-T10 and multichannel bridge implantation in the injury site. Illustrating approximate bridge dimensions. (c) Schematic multichannel bridge regions where the bridge was divided for analysis. From the rostral edge of the bridge/tissue interface, rostral region analysis was done at 300 μm , middle at 900 μm , and caudal at 1600 μm .

Figure. S2. Local delivery of anti-inflammatory cytokine lentiviral vectors alters (a) Leukocyte activation (GO:0045321)-, (b) Inflammatory response (GO:0006954)-, (c) Leukocyte migration (GO:0002685)-, (d) Immune response (GO:0006955)- (e) Neuron differentiation (GO:0030182)- and (f) Synapse organization (GO:0050808)-related gene ontologies at day 7 post-SCI.

Figure. S3. Overexpression of anti-inflammatory cytokines influences the number of M2 phenotypes within the bridges. (a) The transgene expression of IL-10 was associated with the increased number of M2 phenotypes (Pearson coefficient=0.9093; $P<0.0001$; $r^2=0.8268$). (b) Overexpression of IL-4 also correlated to increased number of M2 macrophages at the injury site (Pearson coefficient=0.7067; $P=0.0032$; $r^2=0.4994$).

Figure. S4. In the sub-acute phase, extensive co-localization of MBP⁺ and P0⁺ myelin was observed around and outer surface of multichannel bridges in the rostral position for (a) vIL-10 and (b) vIL-4 (scale bar 50 μm). The dashed lines indicate the interface between bridge implants and spinal cord tissue. (c) Percentage of axons that were myelinated within the bridge area at day 28 post-SCI. No difference was observed between groups. One-way ANOVA with Tukey's post hoc test (mean \pm SEM, $n=5$ /group).

Figure. S5. vIL-10 and vIL-4 delivery increases the number of axons and oligodendrocyte-derived myelinated axons as a function of time at the injury. The total number of axons, oligodendrocyte-derived and Schwann cell-derived myelinated axons were quantified in delivery of (a) bridge only, (b) vCtrl, (c) vIL-10, and (d) vIL-4 in the sub-acute (day 28) and chronic phase (day 84). The statistical tests were completed using a two-way ANOVA with Šidák correction for the multiple comparisons. (* $P<0.05$, ** $P<0.01$ and **** $P<0.0001$, $n=5$ /group)

Figure. S6. Multichannel bridge with anti-inflammatory cytokines improves specific components of locomotion recovery from SCI. (a-d) The BMS subscore in vIL-4 and vIL-10 groups was significantly increased relative to bridge only and vCtrl throughout day 84. Furthermore, bridge itself increased the frequency of plantar stepping and fore limb-hind limb coordination compared to SCI only as a function of time. Statistical test was completed using a one-way ANOVA with Tukey's post hoc test. ^s $P<0.05$, and ^{ss} $P<0.01$ compared to SCI only, and ^{***} $P<0.001$ and ^{****} $P<0.0001$ compared to vCtrl; mean \pm SEM and $n=15$ /group

Table S1. Gene ontology accession number

Name	Accession Number
Inflammatory response	GO:0006954
Leukocyte activation	GO:0045321
Nervous system development	GO:0007399
Locomotor behavior	GO:0007626
Synapse organization	GO:0050808
Immune system process	GO:0002682
Leukocyte migration	GO:0002685
Immune response	GO:0006955
Neuron differentiation	GO:0030182
Chemical synaptic transmission	GO:0007268

Table S2. Primer sequences for qRT-PCR

Gene	Accession number (GenBank)	Forward (5'-3')	Reverse (5'-3')
Ii7r	NM_008372.4	GCTGTACACAGTGCAAACCG	GTGGAGATGGGCTGTCTCTG
Cd28	NM_007642.4	TGGCTTGCTAGTGACAGTGG	CATTGGTGGCCCAGTAGAGG
Cdk6	NM_009873.3	GCATCGTGATCTGAAACCGC	CCACGTCTGAACTTCCACGA
Arginase1	U51805.1	GAACACGGCAGTGGCTTTAAC	TGCTTAGCTCTGTCTGCTTTGC
CD206	NM_008625.2	TCTTTGCCTTTCCAGTCTCC	TGACACCCAGCGGAATTTCC
Retnla	NM_020509.3	GGTCCCAGTGCATATGGATGAGACCATAGA	CACCTCTTCACTCGAGGGACAGTTGGCAGC
CD86	NM_019388.3	TTGTGTGTGTTCTGGAAACGGAG	AACTTAGAGGCTGTGTTGCTGGG
iNOS	U58677.1	CCCTTCAATGGTTGGTACATGG	ACATTGATCTCCGTGACAGCC
MHC-II	NM_207105.3	GACGCTCAACTTGTCCCAAAAC	GCAGCCGTGAACTTGTGAAC
18s-rRNA	NR_003278.3	GCAATTATCCCCATGAACG	GGCCTCACTAAACCATCCAA-3
Hoxc10	NM_010462.5	TGTACAGTGCGAGAGAAGCGG	GTGTCTGGACTGGAGTCTGC
Chat	NM_009891.2	GGCTTTTGTGCAAGCCATGA	CACAGGGCCATAACAGCAGA
Efna3	NM_010108.1	CTACATCTCCACGCCCACTC	CCTGGGGATTCTCTCCCTCA
Hapln4	NM_177900.4	GGTCACAAGATGATCGTGCC	TGACCTTAAGAAGCCGAGCA
Trpc5	NM_009428.3	AACTCCCTCTACCTGGCAAC	TTCTGCAATCAGAGTCGGGT
Lhx5	NM_008499.5	CAGGATCCGTTACAGGACGA	AACCACACCTGAATGACCCT
Scn1a	NM_001313997.1	GTGTGCTCAAGCTCATCTCG	GCACCTTTGATCAGGCGTAG
Hoxd10	NM_013554.5	AACCAGCAATTGGCTCACTG	TTACTGATCTCTAGGCGGCG
Negr1	NM_177274.4	CGGTGCTCAGGTGTTACTTG	GAAACTCGAGGGTCCACTGA